

A NEW IMPLEMENTATION OF SINGLE PHASE SHIMIZU INVERTER FOR OPTIMAL POWER FLOW OF SOLAR PV SYSTEM BASED ON INCREMENTAL CONDUCTANCE MPPT METHOD

FERDIAN RONILAYA, INDRAZNO SIRADJUDDIN, SUNGKONO EKO WIBOWO
AND IMRON RIDZKY

Department of Electrical Engineering
State Polytechnic of Malang
Jalan Soekarno-Hatta, No. 9, Malang 65141, Indonesia
ferdian@polinema.ac.id

Received November 2017; accepted February 2018

ABSTRACT. *This paper presents a new implementation of flyback-type inverter to optimize power flow from solar PV (photovoltaic) system. The flyback-type inverter used is Shimizu topology. The main features of this inverter type include: extended lifetime of the inverter, providing small volume, lightweight, lower harmonic content and stable AC current injection into the load or utility line. Three controllers used comprise non-MPPT, conventional Incremental Conductance (IC) and IC+PID method. To verify the effectiveness of the inverter design, such methods are examined with different irradiance conditions. The results show that the Shimizu flyback-type inverter exhibits considerable optimum performance and can harvest a good maximum power under various irradiance condition. The results also indicate that the IC+PID method gives less harmonic distortion.*

Keywords: Flyback-type inverter, Incremental conductance, Maximum power point tracker, Photovoltaic, PID, Total harmonic distortion

1. **Introduction.** Renewable energy is becoming increasingly popular in today's world since fossil energy reserve is limited. The solar photovoltaic is probably the most popular renewable sources in Indonesia. Indonesia is located in the equatorial line, which is characterized by having heavy rain, constant high temperature and relatively high humidity. On the average, the solar irradiance for Indonesia is around 4.8 kWh/m²/day [1]. However, it is hard to get a clear sky without sun-shading even in period of the dry season (July-October). The solar photovoltaic panel could be then completely or partially covered by cloud, thus decreasing its power output. Furthermore, this can reduce the solar panel's efficiency. Hence, if the solar irradiance is low, we should find the new point at which the PV panel operates at its maximum power point so that we can harvest as much energy as possible.

Various inverter topologies have been proposed by many researchers. In a conventional PV array system, PV modules are connected in series to get suitable DC voltage and then convert it to AC voltage through an inverter. However, when shading occurs in PV modules, the total power generated decreases significantly. Strategy of AC module is used to overcome this problem. A small interactive inverter is installed on each single PV module. The output of each inverter is then connected in parallel. This configuration may improve the flexibility of PV power flow control. It requires an inverter that is light-weight, small in size, low cost and high in efficiency. To meet these requirements, a flyback inverter may offer some advantages as follows [2-5]: it does not require DC-DC converter for MPPT operation, it employs less number of power switches, the use

of high frequency transformer may reduce inverter size and may also provide isolation, and it operates at unity power factor when it is connected to a grid. Based on the literature review, it is reported that flyback-type inverter research focuses on three main issues: efficiency enhancement [3,5-9], capacitor size reduction [2,10-12] and optimal power harvesting through MPPT method development. A sensorless current MPPT used with a flyback-type inverter can be found in [13,14]. The proposed method is realized with PV current estimations from the capacitor voltage which is connected in parallel with the PV array. However, the algorithm used to estimate the PV current is complex because it requires an interrupt routine program that should be reset to zero and is repeated after a determined repetition rate. The use of Perturb and Observe (P&O) MPPT method can be found in [15,16]. However, the major disadvantage of P&O method is that rapid change in atmospheric condition may decrease the MPPT performance. Furthermore, the P&O method may cause high spikes and then can damage the equipment [17].

This paper proposes a new implementation of Shimizu inverter for optimal power flow of solar PV system by using incremental conductance algorithm. To the best of our knowledge, there are quite a few papers discussing the similar topic, previously. The inverter is capable of handling power differences between the input and output using a small thin film capacitor and the controller uses a simple algorithm.

The organization of this paper is as follows. Section 2 describes the theoretical framework of Shimizu inverter. Section 3 discusses an incremental conductance algorithm that is used as the optimal power flow control method. Results and discussion are given in Section 4 and finally, Section 5 presents the conclusion.

2. A Circuit Configuration of Shimizu Inverter.

2.1. Circuit topology and operation of Shimizu inverter. The circuit of Shimizu inverter is shown by Figure 1. As we can see, the main components of this inverter

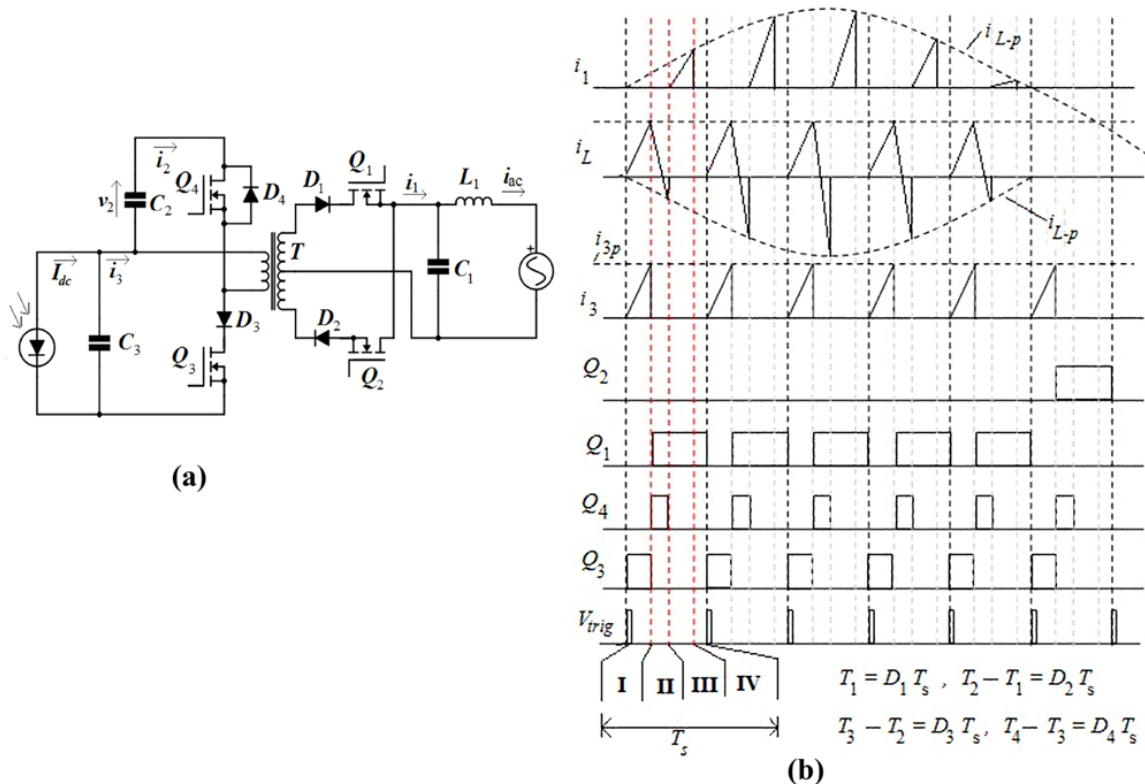


FIGURE 1. (a) The circuit topology of Shimizu inverter and (b) the operation principle of Shimizu inverter

comprise two main switches (Q_3 and Q_4), a center-taped flyback transformer (T_1), AC switches (Q_1 and Q_2), C - L filter, input capacitor (C_3), and capacitor in power smoothing circuit (C_2). The series-connected diodes (D_1 , D_2 , and D_3) are used to block reverse current. D_4 represents the body diode of MOSFET Q_4 . The size of transformer T_1 is relatively small since the switching frequency is set at 20 kHz.

Q_1 and Q_2 are ON during positive and negative cycles, respectively. Meanwhile, Q_3 and Q_4 are operated in ZCS (zero current switching) or ZVS (zero voltage switching) and the magnetizing current of T_1 is worked under a discontinuous mode. The operation principle of this inverter is described by Figure 1, and is explained as follows [2].

Mode I:

When Q_3 is ON and Q_1 , Q_2 , Q_4 are OFF, the current i_3 will increase linearly and the maximum current is given by:

$$i_{3p} = (i_3(nT_s + T_1)) = \frac{E_{dc}T_1}{L_p} = \frac{E_{dc}D_1T_s}{L_p} \tag{1}$$

where E_{dc} : input voltage, L_p : inductance of primary winding, n : the coefficient factor and T_1 : ON time duration of switch Q_3 , D_1 is the duty cycle at Mode I and T_s represents the switching interval. In this mode, $i_3 = i_L$.

Mode II:

As Q_3 is OFF and the switches Q_4 and Q_1 (or Q_2) are ON, the direction of magnetizing current, i_L , is reversed. If the amplitude of oil is equal to i_{L-p} (as shown in Figure 1) the switch Q_4 is OFF. So, the duty cycle D_2 during this mode can be computed as:

$$D_2 = \frac{L_p}{v_2T_s}(i_{L-p} + i_{3p}) \tag{2}$$

with v_2 : capacitor voltage, i_{L-p} : peak current of i_L . Because of ZCS behavior, the diode D_1 will be OFF as i_1 decreases to zero.

Mode III:

In this mode, a current, i_1 , flows from one of secondary windings L_s through switch Q_1 or Q_2 . It is assumed that the grid voltage during switching interval (T_s) is constant and then the absolute value of i_1 is computed by (3).

$$|i_1(t)| = \left| \frac{i_{L-p}}{N} - \frac{v_{ac}}{L_s}[t - (nT_s + T_2)] \right| \tag{3}$$

where $N = \sqrt{L_s/L_p}$ and $t = nT_s + T_3$. Hence, the duty ratio during Mode III is expressed by the following equation:

$$D_3 = \frac{I_{L-p}L_pN}{v_{ac}T_s} \tag{4}$$

Mode IV:

In this mode, there is no current flowing from/to the transformer. A low pass filter (LPF) C_1 - L_1 is used to eliminate high frequency components in the current i_1 so that the average value of i_1 is expressed by (5).

$$|\bar{i}_1| = \frac{1}{T_s} \int_{nT_s+T_2}^{nT_s+T_3} i_1(t)dt = \frac{L_p(i_{L-p})^2}{2T_s v_{ac}} \tag{5}$$

v_{ac} and i_{L-p} are defined as follows:

$$v_{ac} = V_{ac}|\sin \omega t| \quad i_{L-p} = I_2|\sin \omega t| \tag{6}$$

Substituting Equation (6) to (5), we can get:

$$|\bar{i}_1| = \frac{L_p(I_2)^2}{2T_s V_{ac}}|\sin \omega t| \tag{7}$$

As we can see in Figure 1, V_{trig} determines the operation of the switches Q_1 and Q_2 and hence influences the polarity of current $i_1(t)$. From this, we can write the AC current injected to the grid as follows:

$$i_{ac}(t) = \frac{L_p(I_2)^2}{2T_s V_{ac}} \sin \omega t \quad (8)$$

2.2. Determining optimum circuit parameters. To get the sufficient magnetizing current i_L , the value of voltage v_2 must be positive so that the amplitude of V_2 should be lower than $V_{2(dc)}$ as expressed as:

$$V_{2\min} = V_{2(dc)} - V_x = -2V_{2(dc)} + \sqrt{V_{2(dc)}^2 + \frac{V_{ac}I_{ac}T_{ac}}{4\pi C_2}} \quad (9)$$

where

$$V_2 = -V_{2(dc)} + \sqrt{V_{2(dc)}^2 + \frac{V_{ac}I_{ac}T_{ac}}{4\pi C_2}} \quad (10)$$

As suggested by Shimizu et al. in [2], the optimum value of L_p can be calculated using (11).

$$L_p < \frac{T_s}{V_{ac}I_{ac}} \times \left(\frac{E_{dc}V_{ac}V_2}{E_{dc}V_2 + (1 + \sqrt{2} \sin \omega t) E_{dc}V_{ac} + NE_{dc}V_{ac}} \right)^2 \quad (11)$$

In general, the minimum value of V_2 occurs at $\omega t = \theta = 3\pi/4$. Hence, Equation (11) can be rearranged as follows:

$$L_p < \frac{T_s}{V_{ac}I_{ac}} \left(\frac{E_{dc}V_{ac}V_{2\min}}{E_{dc}V_{2\min} + 2E_{dc}V_{ac} + NE_{dc}V_{ac}} \right)^2 \quad (12)$$

3. Incremental Conductance Method for Shimizu Inverter.

3.1. Incremental Conductance (IC) method. The main components used in the incremental conductance method are voltage and current sensors. It is used to measure voltage and current of the PV array. By using this method, the output voltage of the PV array is conditioned such that the maximum power point is obtained.

Figure 2(a) shows the working operation of IC technique and the flowchart the IC method is shown by Figure 2(b). At Maximum Power Point (MPP) the value of dP/dV is equal to zero. The basic formula for IC technique is given as follows [18]:

$$\begin{aligned} \frac{dI}{dV} &= -\frac{I}{V}, \text{ at MPP} \\ \frac{dI}{dV} &> -\frac{I}{V}, \text{ at the left side of MPP} \\ \frac{dI}{dV} &< -\frac{I}{V}, \text{ at the right side of MPP} \end{aligned} \quad (13)$$

V and I are the output voltage and current of solar panel, respectively. From Equation (13), incremental conductance is represented by the left side of that equation, whereas, the right side represents instantaneous conductance. The MPPT unit controls the PWM signal (V_{ref}) of the converter such that the following condition is met:

$$\frac{dI}{dV} + \frac{I}{V} = 0 \quad (14)$$

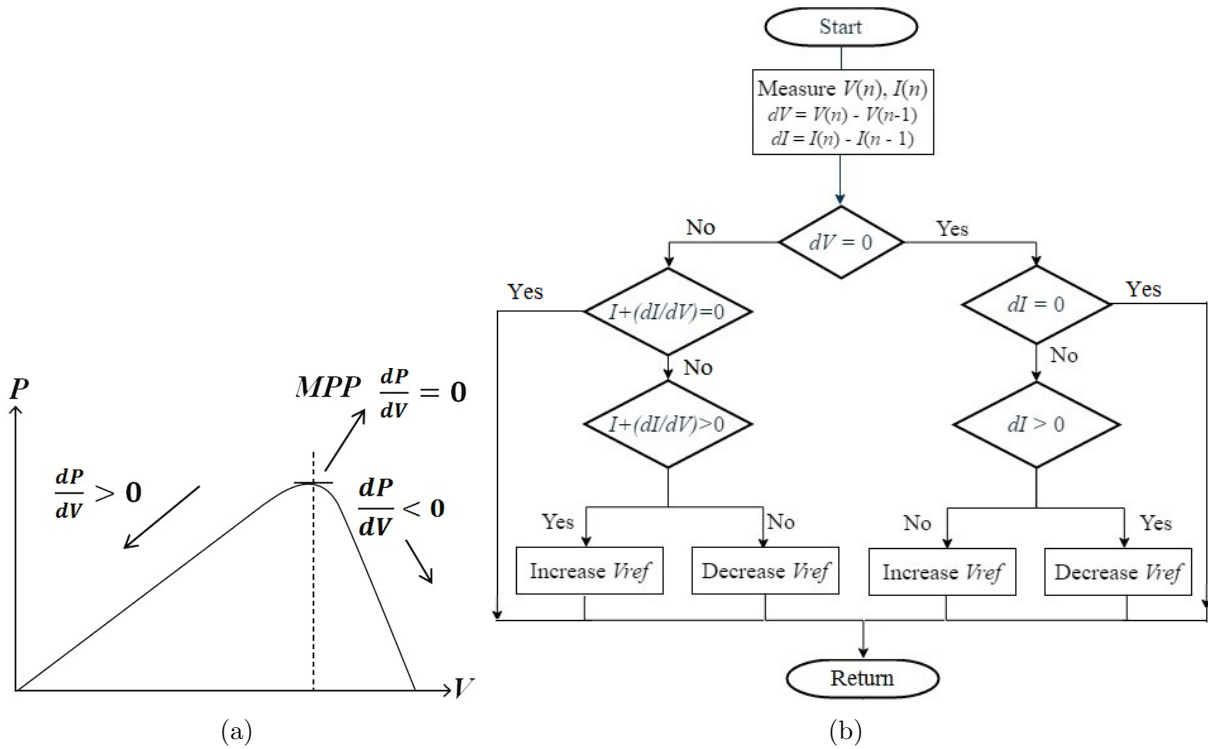


FIGURE 2. (a) Working principle of IC method on a P-V curve and (b) the algorithm of the IC method

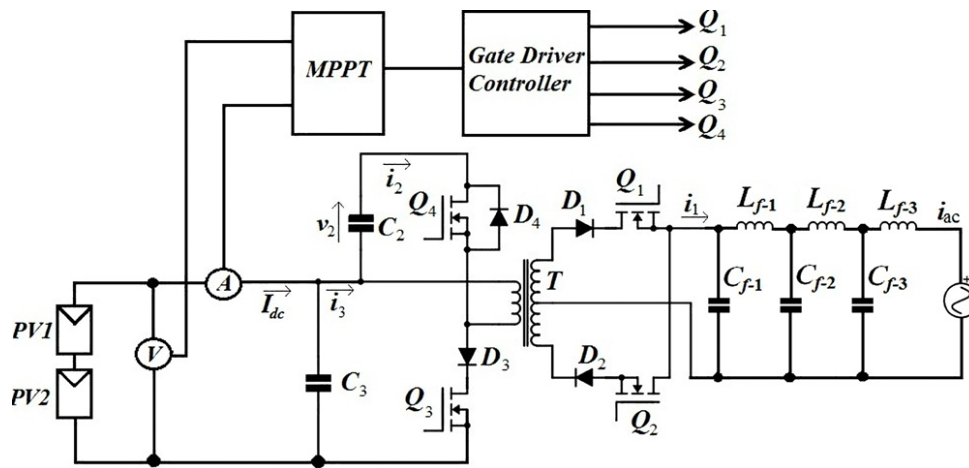


FIGURE 3. The investigated inverter circuit topology

3.2. **A design of IC algorithm for Shimizu inverter.** Figure 3 depicts the circuit topology of the inverter. The circuit parameters used are listed in Table 1. The controller circuit for the inverter is shown by Figure 4(a). i_{3p} is the maximum output current of the solar panel and is obtained from an MPPT block as given in Figure 4(b). Meanwhile, i_3 is the current flowing to the primary coil of the transformer. These two currents are then used to execute the turn-on or off action of MOSFET Q_3 . The on/off state of those two MOSFET is determined by V_{trig} which has 20 kHz of switching frequency. i_{L-p} determines the maximum recharge value of primary coil inductor obtained from Equation (15) whereas i_L is the instantaneous value while inductor is recharged. Both currents are used to drive MOSFET Q_4 . Switching signal for Q_1 and Q_2 depends on v_{ac} and the output signal of Q_3 .

$$i_{L-p} = i_{3p} \sqrt{2} \sin \omega t \tag{15}$$

TABLE 1. The circuit parameters

| | | |
|--------------------------------|---------------------|---------------|
| PV voltage | E_{dc} | 16.09-19.72 V |
| Switching frequency | f_s | 20 kHz |
| DC input capacitor | C_3 | 80 μ F |
| Decoupling capacitor | C_2 | 40 μ F |
| AC filter inductor | $L_{f-1} - L_{f-3}$ | 27 mH |
| AC filter capacitor | $C_{f-1} - C_{f-3}$ | 12.4 mF |
| Primary inductance of T_1 | L_p | 23.87 μ H |
| Secondary inductance of T_1 | L_s | 1.492 μ H |
| The gain of PID | K_p | 2.46 |
| The integral constant of PID | T_i | 0.000982 |
| The derivative constant of PID | T_d | 35 |

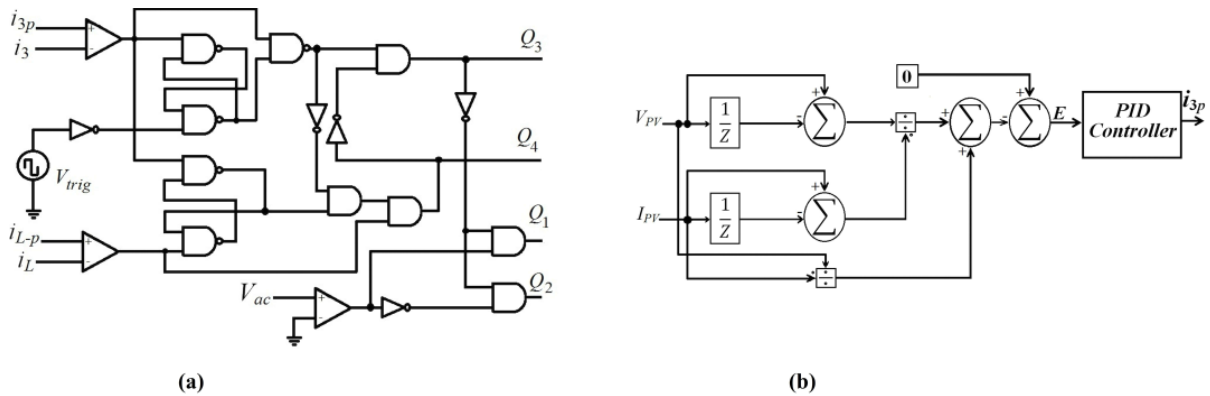


FIGURE 4. (a) The Shimizu inverter controller and (b) the model of IC MPPT technique

The MPPT algorithm used in this paper is IC method and the model is given by Figure 4(b). To ensure an optimal power flow from solar PV, a PID controller is used. The output of this MPPT block is i_{3p} and then is used as reference value for the inverter controller.

4. Results and Discussion. To verify the effectiveness of the proposed system, several simulation experiments are performed under various irradiance conditions, i.e., 250 W/m², 500 W/m² and 750 W/m².

Figure 5(a) shows the output voltage waveform of the inverter measured before the AC filter. As we can see that it contains high frequency switching component with 20 kHz as indicated in Figure 5(b). From Figure 5(b), i_3 will be kept constant according to the maximum P-V capability. This operation is handled by the IC MPPT block. When Q_3 is active, the primary winding of the transformer will be charged to maximum limit of i_{3p} . Then, Q_3 is off and i_2 flows in the opposite direction through C_2 , Q_4 and L_p . When Q_1 or Q_2 is on, energy in the flyback transformer will be released to the grid.

The AC output voltage profile after the AC filter is given by Figure 6(a). Since V_{ac} and I_{ac} are in phase, the inverter gives unity power factor. Figure 6(b) depicts the voltage and current profiles at the DC side of the inverter. These two values are maintained constant. This figure depicts that the voltage across the decoupling capacitor C_2 has a frequency that is twice as high as grid frequency.

The output PV power response under various irradiance conditions is shown by Figure 7. The non-MPPT controller system exhibits worse performance as it delivers less power compared with that of conventional IC and IC+PID MPPT method. An improved power

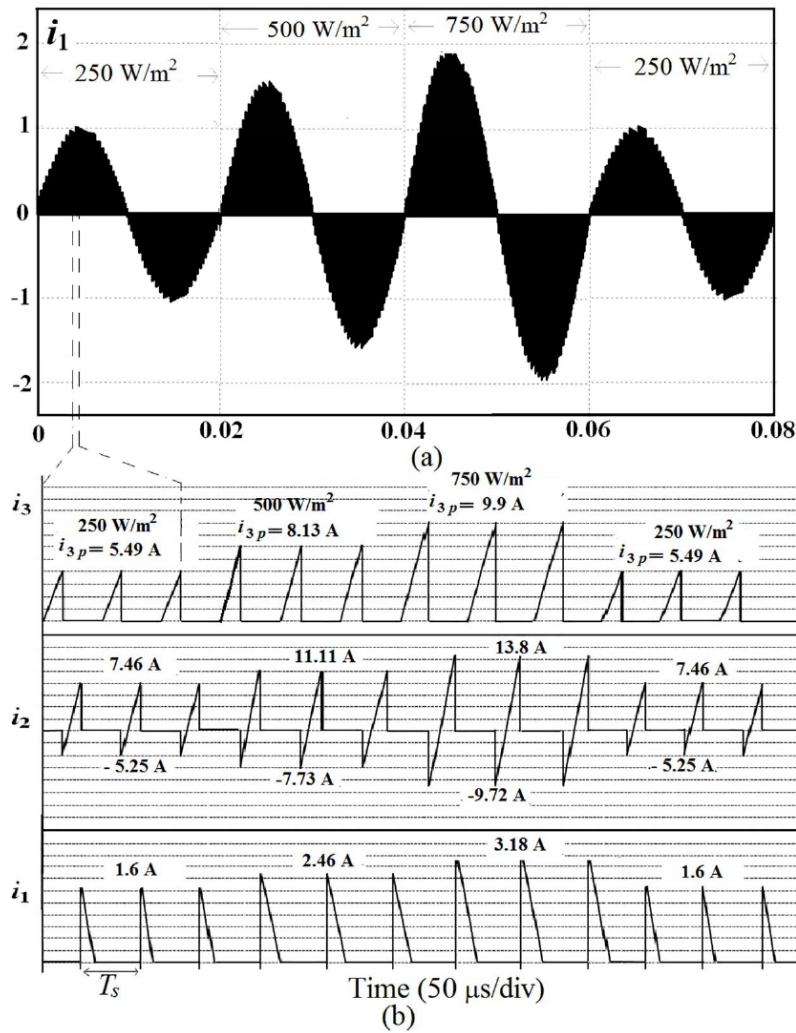


FIGURE 5. (a) The output waveform before the filter and (b) the waveforms at some switching periods

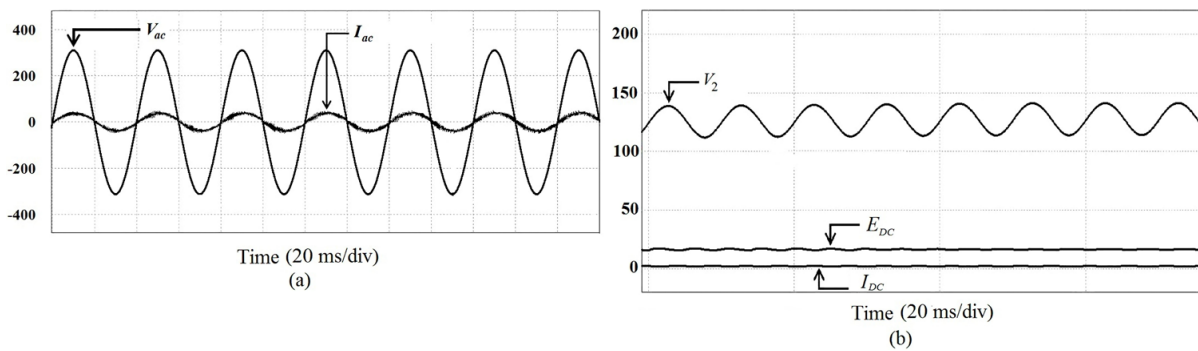


FIGURE 6. (a) The AC output voltage and current after the filter and (b) voltage and current profiles at DC side of the inverter at 250 W/m²

profile is obtained when the IC+PID MPPT method is used. This method may significantly increase the PV power to be delivered at around 5 times higher than non-MPPT technique.

The Total Harmonic Distortion (THD) for different control methods is listed in Table 2. It can be clearly seen that the IC+PID provides lower current THD. The lower the irradiance is, the higher the THD is. Meanwhile, the non-MPPT cannot give an optimum power harvesting as it is indicated by Figure 7. The harmonic current profiles for different

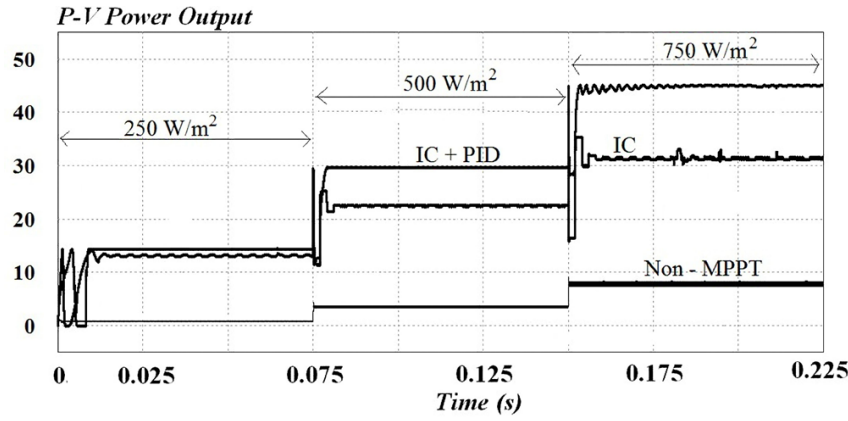


FIGURE 7. The PV power under various irradiance and control methods

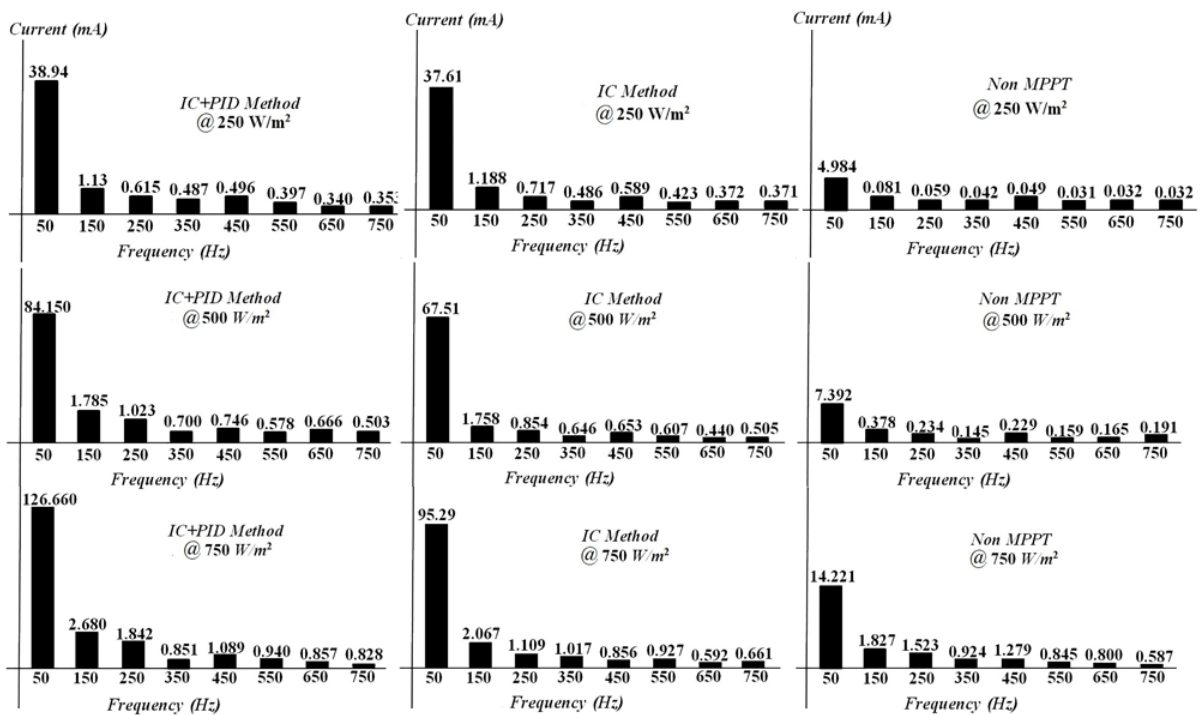


FIGURE 8. The current harmonic spectrum

TABLE 2. The THD of current profiles

| Irradiance (W/m ²) | Non-MPPT | IC Method | IC+PID Method |
|--------------------------------|----------|-----------|---------------|
| 250 | 2.62% | 4.58% | 4.09% |
| 500 | 8.13% | 3.47% | 2.99% |
| 750 | 22.06% | 3.13% | 3.04% |
| Average value | 10.94% | 3.73% | 3.37% |

irradiance and controller methods are given in Figure 8. This figure confirms that the harmonic profile for the IC+PID is lower than the other two methods. It reveals that the use of IC+PID method for MPPT of the PV panel may offer stable current injection. Moreover, the results indicate that IC+PID method provides less ripple current.

5. Conclusion. The design of Shimizu inverter for optimal power flow from solar PV has been discussed. To verify the effectiveness of the design, the inverter is examined

under various irradiance conditions, i.e., 250 W/m², 500 W/m² and 750 W/m². The controllers used to execute the design include non-MPPT, IC and IC+PID methods. The results show that the designed-inverter exhibits considerable optimum performance and can harvest a good maximum power under various irradiance conditions. The results also indicate that the IC+PID method has less harmonic distortion compared with the other two controller methods.

On the theoretical side, the results of the presented approach in this paper are based on a simulation case study. Much remains to be done in this regard and hence additional work will be required to know the real system performance, especially when the system is fully hardware-implemented.

Acknowledgment. This research project was supported by the State Polytechnic of Malang (grant number: 042.01.2.401004/2017).

REFERENCES

- [1] R. I. Putri, S. Wibowo and M. Rifa'i, Maximum power point tracking for solar panel using incremental conductance method, *The 2nd International Conference on Sustainable Energy Engineering and Application*, 2014.
- [2] T. Shimizu, K. Wada and N. Nakamura, Flyback-type single-phase utility interactive inverter with power pulsation decoupling on the DC input for an AC photovoltaic module system, *IEEE Trans. Power Electronics*, vol.21, no.5, pp.1264-1272, 2006.
- [3] G. Tan, J. Wang and Y. Ji, Soft-switching flyback inverter with enhanced power decoupling for photovoltaic applications, *Electric Power Applications*, vol.1, no.2, pp.264-274, 2007.
- [4] A. C. Kyritsis, E. Tatakis and N. Papanikolaou, Optimum design of the current-source flyback inverter for decentralized grid-connected photovoltaic systems, *IEEE Trans. Energy Conversion*, vol.23, no.1, pp.281-293, 2008.
- [5] F. Zhang and C. Gong, A new control strategy of single-stage flyback inverter, *IEEE Trans. Industrial Electronics*, vol.8, no.56, pp.3169-3173, 2009.
- [6] Y.-H. Kim, Y.-H. Ji, J.-G. Kim, Y.-C. Jung and C.-Y. Won, A new control strategy for improving weighted efficiency in photovoltaic AC module-type interleaved flyback inverters, *IEEE Trans. Power Electronics*, vol.28, no.6, pp.2688-2699, 2013.
- [7] N. Suresh, M. Pahlevaninezhad and P. K. Jain, Analysis and implementation of a single-stage flyback pv microinverter with soft switching text, *IEEE Trans. Industrial Electronics*, vol.61, no.4, pp.1819-1833, 2014.
- [8] A. C. Nanakos, G. C. Christidis and E. C. Tatakis, Weighted efficiency optimization of flyback microinverter under improved boundary conduction mode (i-BCM), *IEEE Trans. Power Electronics*, vol.30, no.10, pp.5548-5564, 2015.
- [9] G. C. Christidis, A. C. Nanakos and E. C. Tatakis, Hybrid discontinuous/boundary conduction mode of flyback microinverter for AC PV modules, *IEEE Trans. Power Electronics*, vol.31, no.6, pp.4195-4205, 2016.
- [10] S. Zengin, F. Deveci and M. Boztepe, Decoupling capacitor selection in DCM flyback PV microinverters considering harmonic distortion, *IEEE Trans. Power Electronics*, vol.28, no.2, pp.816-825, 2013.
- [11] H. Hu, S. Harb, N. H. Kutkut, Z. J. Shen and I. Batarseh, A single-stage microinverter without using electrolytic capacitors, *IEEE Trans. Power Electronics*, vol.28, no.6, pp.2677-2687, 2013.
- [12] J.-G. Kim, K.-D. Kim, Y.-S. Noh, Y.-C. Jung and C.-Y. Won, Analysis and design of a three-port flyback inverter using an active power decoupling method to minimize input capacitance, *Journal of Power Electronics*, vol.13, no.4, pp.558-568, 2013.
- [13] N. Kasa, T. Iida and L. Chen, Flyback inverter controlled by sensorless current MPPT for photovoltaic power system, *IEEE Trans. Industrial Electronics*, vol.52, no.4, 2005.
- [14] B.-Y. Choi, J.-W. Jang, Y.-H. Kim, Y.-H. Ji, Y.-C. Jung and C.-Y. Won, Current sensorless MPPT using photovoltaic AC module-type flyback inverter, *IEEE International Symposium on Industrial Electronics (ISIE)*, pp.1-6, 2013.
- [15] T. Shimizu, K. Wada and N. Nakamura, A flyback-type single phase utility interactive inverter with low-frequency ripple current reduction on the DC input for an AC photovoltaic module system, *IEEE the 33rd Annual Power Electronics Specialists Conference*, vol.3, pp.1483-1488, 2002.
- [16] B. Tamyurek and B. Kirimer, An interleaved high-power flyback inverter for photovoltaic applications, *IEEE Trans. Power Electronics*, vol.30, no.6, 2015.

- [17] B. Subudhi and R. Pradhan, A comparative study on maximum power point tracking techniques for photovoltaic power systems, *IEEE Trans. Sustainable Energy*, vol.4, no.1, pp.89-98, 2013.
- [18] S. Sumathi, L. A. Kumar and P. Surekha, *Solar PV and Wind Energy Systems: An Introduction to Theory, Modelling with Matlab/Simulink and the Role of Soft Computing Techniques*, Springer International Publishing, Switzerland, 2015.